DOI: 10.1002/asia.201100217

Solubilization of Polycyclic Aromatics in Water by γ-Cyclodextrin Derivatives

Hai Ming Wang and Gerhard Wenz*[a]

Abstract: A series of hydrophilic per-6-thio-6-deoxy-γ-cyclodextrins (CDs) were synthesized from per-6-iodo-6-deoxy-γ-CD. These new hosts are able to solubilize polycyclic aromatic guests in aqueous solution to much higher extents than native CDs. Phase-solubility diagrams were mostly linear in accordance with both 1:1 and 1:2 CD–guest complexes in aqueous solution. The stoichiometry of the inclusion complexes was further investigated by fluorescence spectroscopy, which revealed very pronounced Stokes shifts typical for 1:2 complexes. This finding was further consolidated by quantum mechanical calculations of dimer formation of the guests and space-filling considerations by using the cross-sectional areas of the CDs and guests. The calculated dimerization energies correlated well with the binding free energies measured for the 1:2 complexes, and provided the main contribution to the driving force of complexation in the γ-CD cavity.

Keywords: cyclodextrins · dimerization · fluorescence · inclusion compounds · polycycles

Introduction

Cyclodextrins (CDs) are a series of cyclic oligosaccharides. They consist of α-1,4-linked glucose subunits that form hollow truncated cones of various diameters.[1] Those CDs, composed of six, seven, and eight glucose units, are produced on industrial scales and called α-, β-, and γ-CDs, respectively. On account of their unique molecular structure, CDs and their derivatives have the remarkable ability to accommodate a wide variety of guest molecules in aqueous solution by means of noncovalent interactions.[2] This property is currently used in numerous applications in pharmaceutical, food, and chemical industries, and is also extensively exploited to improve the efficiency and selectivity of chemical reactions.[3] Many efforts are now dedicated to the improvement of solubility, stability, reactivity, and other properties of guest molecules by complexation in CDs and CD derivatives.[2b,4]

Composed of a hydrophilic shell and a relatively hydrophobic cavity, CDs solubilize hydrophobic organic compounds through the formation of water-soluble inclusion complexes mainly driven by hydrophobic interaction.[3c,5] There are indeed many reports on the solubility enhancements of hydrophobic or amphiphilic guests, including pharmaceutical drugs, by CDs in aqueous solution.[3c,6] But, due to the limited water solubilities of native CDs, the solubility enhancements reached by native CDs are generally small. However, modifications on the free hydroxyl groups of native CDs with appropriate functional groups[5b,7] may not only significantly increase the water solubility of CDs, but also greatly increase the ability of CDs to form inclusion complexes with guest molecules. For instance, methylated β-CD and 2-hydroxypropyl-β-CD are superior in the solubilization of drugs relative to native β-CD.[5b] CD sulfonates[8] perform even better than the neutral derivatives, especially for the solubilization of hydrophobic guests such as naphthalene (NAP) in water.[7a] Recently, we found a new class of hydrophilic per-6-deoxy-thioethers of β-CD, which showed exceptionally high binding constants ($K > 10^6\,\mathrm{M}^{-1}$, equivalent to $\Delta G < -34\,\mathrm{kJ\,mol}^{-1}$) for *para*-disubstituted benzene derivatives in water. The higher hydrophobicity of sulfur compared to oxygen, which leads to an extension of the hydrophobic cavity, and additional Coulomb interactions, were supposed to be responsible for the observed high binding potentials of these hosts.[2c,9]

[a] H. M. Wang, Prof. Dr. G. Wenz
Organische Makromolekulare Chemie
Saarland University
Geb. C4.2, 66123 Saarbrücken (Germany)
Fax: (+49) 681-302-3909
E-mail: g.wenz@mx.uni-saarland.de

Supporting information for this article is available on the WWW under http://dx.doi.org/10.1002/asia.201100217.

Only a few efforts have presently been made to evaluate the capabilities of modified γ-CD for solubility enhancements of guest molecules.[10] It is known that γ-CD is able to accommodate two aromatic guests simultaneously within its relatively large cavity, thereby leading to an inclusion compound with 1:2 stoichiometry.[2b] Consequently, γ-CD and its derivatives are very interesting nanovessels for the execution of various bimolecular reactions, especially cycloadditions.[11] For instance, Nakamura and Inoue reported that the host–guest ratio in the inclusion complex of γ-CD with 2-anthracene carboxylate in water was 1:2 based on the results from ROESY-NMR spectroscopy measurements.[12] Also the ROESY-NMR spectrum of the inclusion system of γ-CD with methyl 3-methoxyl-2-naphthoate demonstrated the existence of a complex with 1:2 stoichiometry.[11c] Accordingly, regio- and stereoselective photodimerizations between two substrates, both in solution and in the solid state, had been achieved in the presence of γ-CD.[11a,k]

In this work we report on the synthesis of highly water-soluble thioethers of γ-CD with flexible neutral or ionic side arms, because we hoped that this derivatization might lead to a similar enhancement of the binding potential like that observed for β-CD thioethers.[2a,c]

Eight polycyclic aromatics of similar size (see Scheme 1): napthalene (NAP), 2-naphthalenecarboxylic acid (NCA), azulene (AZU), *trans*-stilbene (STI), acenaphthylene (ACE), anthracene (ANT), phenanthrene (PHE), and tetracene (TET) were chosen as guests to study the solubility enhancements and both stabilities and stoichiometries of the complexes. It should be noted that some of the aromatic guests such as STI and ANT can serve as candidates for photodimerization reactions.

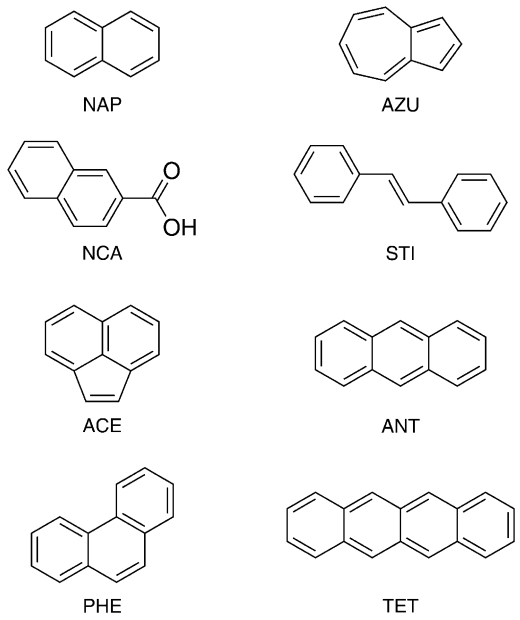

Scheme 1. Chemical structures of the selected polycyclic aromatic guests: naphthalene, NAP; 2-naphthalenecarboxylic acid, NCA; azulene, AZU; *trans*-stilbene, STI; acenaphthylene, ACE; anthracene, ANT; phenanthrene, PHE; tetracene, TET.

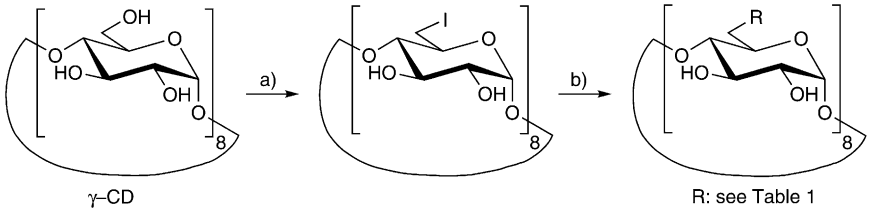

Scheme 2. Synthesis of octasubstituted γ-CD thioethers: a) 1) PPh_3, I_2, DMF; 2) Ac_2O, pyridine; 3) NaOMe, MeOH; b) the corresponding thiol compound, triethylamine, DMF.

Results and Discussion

Synthesis and Characterization

Hydrophilic thioethers **1**–**8** at all primary carbon atoms of γ-CD were synthesized from octakis(6-deoxy-6-iodo)-γ-CD[13] as shown in Scheme 2. For the purpose of a rigorous purification, the octakis-iodo derivative was completely acetylated, subjected to flash chromatography, and deacetylated again. The target compounds were synthesized by nucleophilic displacement reactions in good yields. The reaction proceeded efficiently, and subsequent selective precipitation of the desired product in proper organic solvent allowed the isolation of the octakis-γ-CD derivative. The structures of γ-CD derivatives were characterized by NMR spectroscopy and electrospray ionization mass spectrometry (ESI-MS). Further purifications of these compounds were achieved by nanofiltration in water. Except for derivative **7**, all other synthesized neutral and ionic γ-CD derivatives showed very high water solubilities. The structures of the substituents R, the obtained yields, and the aqueous solubilities of γ-CD derivatives **1**–**8** are summarized in Table 1.

Abstract in Chinese:

合成了一系列亲水八-(6-硫代-6-去氧)-γ-环糊精(CD)。和未取代 CD 比较，新合成主体的存在能够较大程度的增加多环芳烃客体分子在水中的溶解度。相溶解度研究表明在水中形成了 1:1 以及 1:2 型主客体包合物。荧光光谱法以及分子模拟的结果均证实了 1:2 型包合物的存在。理论计算结果表明包合物形成的驱动力主要由多环芳烃客体聚合能提供。多环芳烃客体聚合能的大小和它们与 CD 所形成 1:2 型包合物的结合自由能顺序相一致。

Solubility Studies

Aqueous solubilities of the eight aromatic guests (shown in Scheme 1) were measured by UV/Vis spectroscopy as functions of the concentrations of hosts. These solubilities in the presence of native CDs and γ-CD derivatives for a fixed

Table 1. Substituents R, yields, and solubilities of the synthesized γ-CD derivatives in g/100 g water at 25 °C.

No.	R	Yield [%]	Solubility [%]
1		71	21
2		62	40
3	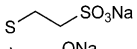	92	49
4	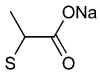	41	42
5	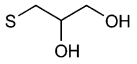	85	22
6	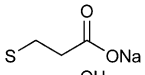	82	24
7		86	0.3
8	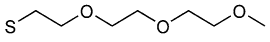	81	48

host concentration of 6 mM, as well as the intrinsic water solubilities of the guests, are listed in Table 2. Although the solubility enhancements caused by native CDs were quite small, significant enhancements were found for the thioethers, thereby revealing very strong intermolecular interactions between CD derivatives **1**–**8** and these aromatic guests in water. In particular, the solubilities enhancements for NAP, AZU, and ANT are much higher than for known CD derivatives like hydroxypropyl-β-CD.[10c] The ionic hosts **1**, **3**, and **6** generally performed better than the neutral ones **5**, **7**, and **8**. Most systems show a linear increase of solubility with host concentrations, displayed in bold characters in Table 2, whereas a few systems show nonlinear solubility enhancements, displayed in italic characters.

The examination of so-called phase-solubility diagrams is widely used to investigate both the complex stoichiometry and binding constants of host–guest complexes. A phase-solubility diagram is obtained by plotting the observed concentration of dissolved guest versus the total concentration of host in solution. According to Higuchi and Connors, they are divided into two main categories, type A and B.[14] Type-A curves, which indicate the formation of soluble inclusion complexes, are obtained when the solubility of the guest increases with increasing CD concentration over the entire concentration range. A linear (A_L-type) relationship is distinguished from positively (A_P-type) or negatively (A_N-type) deviating isotherms. B_s-type and B_I-type phase-solubility diagrams represent the formation of complex with limited solubility and insoluble complex, respectively.

The obtained phase-solubility diagrams are representatively shown in Figure 1. The solubility of PHE increased linearly with the increasing concentrations of native CDs and ionic octasubstituted γ-CD derivatives **3**, **4**, and **6**, thus leading to an A_L type of classification, shown in Figure 1a. On the other hand, curved phase-solubility diagrams were obtained for the complexes of NCA in α-CD and γ-CD derivative **1**, shown in Figure 1b. NCA exhibited a B_S-type diagram with α-CD in water, possibly due to a limited solubility of the formed inclusion complex.[14b] The diagram of NCA with derivative **1** showed A_N-type curvature, which was attributed to electrostatic interaction between the amino groups of **1** and the carboxyl group of NCA, which might lead to aggregation of the CD inclusion complex at higher concentrations.[14b,15] Nevertheless, most complexes in Table 2 show the linear A_L-type phase-solubility diagrams, which can be interpreted by the formation of soluble 1:1, as well as 1:2 host–guest complexes.[14a,16] The complex stoichiometry remained an open question.

Table 2. Intrinsic water solubilities of guests and equilibrium solubilities of guests in 6.0 mM solutions of native CDs and γ-CD derivatives **1**–**8**.[a]

Host	Guest [μM]							
	NAP	NCA	AZU	STI	ACE	ANT	PHE	TET
water	**189**	**322**	**1.4**	**0.6**	**67**	**0.4**	**0.6**	**0.2**
α-CD	**205**	**913**	**26**	*5.0*	*85*	**2.4**	**1.9**	**0.2**
β-CD	*234*	*1460*	*65*	*17*	*105*	**4.6**	**45**	**0.3**
γ-CD	*196*	*431*	**31**	**1.5**	*103*	**1.6**	**5.9**	**0.5**
1	**2440**	*6180*	**588**	**67**	**898**	**44**	**102**	**8.9**
2	**479**	*11400*	**320**	**13**	**729**	**15**	**60**	**5.5**
3	**1590**	**3570**	**841**	**23**	**1703**	**13**	**100**	**6.8**
4	**481**	**9850**	**149**	**13**	**693**	**6.9**	**64**	**5.0**
5	*258*	**2180**	**390**	**14**	**278**	**7.4**	*56*	**3.2**
6	**1080**	**3420**	**670**	**22**	**1280**	**12**	**132**	**6.2**
7[b]	*199*	**863**	**20**	**2.0**	*95*	**0.8**	**19**	**0.2**
8	**515**	**1200**	**353**	**50**	**162**	**14**	**62**	**3.2**

[a] Bold characters: A_L-type linear phase-solubility diagram; italic characters: nonlinear phase-solubility diagram. [b] The concentration of CD derivative **7** was only 1.5 mM due to its low water solubility.

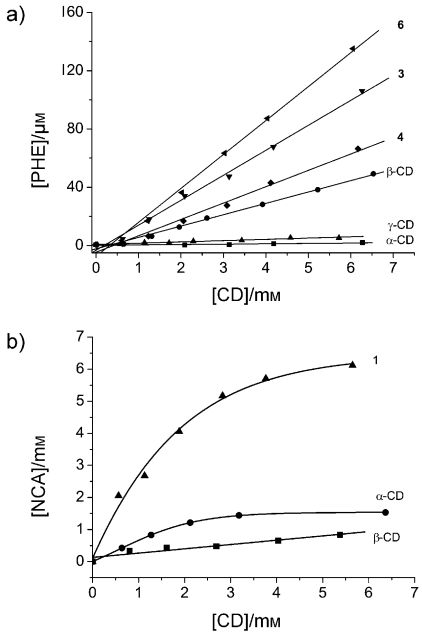

Figure 1. Phase-solubility diagrams for a) PHE and b) NCA in aqueous solution in the presence of native CDs and γ-CD derivatives **6**, **3**, **4**, and **1**.

Complex Stoichiometries

The slope *m* of the phase-solubility diagram, equivalent to the average amount of guest per host, called occupancy, gave some rough idea about the stoichiometry of a complex. These occupancies of γ-CD cavities by the aromatic guests are listed in Table 3. Initial slopes *m* were taken for the curved phase-solubility diagrams.

Occupancy values of more than 100% were found for NCA included in CD derivatives **1**, **2**, and **4**, thereby providing strong evidence for the existence of complexes with 1:2 stoichiometries. An occupancy of less than 100% found in the other cases does not necessarily imply a 1:1 stoichiometry, because cooperativity of inclusion has to be taken into account. If there is a strong interaction between two included guests, a mixture of empty CDs and 1:2 CD complexes will prevail. It should be also noted that several 1:2 complexes with γ-CD or γ-CD derivatives are already known.[11b,c,k,17]

Table 3. Occupancies [%, equal to slope *m*] of aromatic guests within the γ-CD cavity.[a,b]

Host	Guest							
	NAP	NCA	AZU	STI	ACE	ANT	PHE	TET
γ-CD	n.d.	*5.4*	**0.5**	**0.03**	n.d.	**0.02**	**0.09**	n.d.
1	**38**	**165**	**9.7**	**1.2**	**13**	**0.7**	**1.5**	**0.1**
2	**3.9**	**167**	**6.5**	**0.2**	**11**	**0.2**	**1.1**	**0.09**
3	**31**	**55**	**16**	**0.4**	**28**	**0.2**	**1.7**	**0.1**
4	**7.7**	**123**	**2.9**	**0.2**	**11**	**0.1**	**1.2**	**0.08**
5	*12*	**30**	**6.9**	**0.3**	**3.4**	**0.1**	*1.9*	**0.05**
6	**18**	**52**	**12**	**0.4**	**21**	**0.2**	**2.3**	**0.1**
7	*30*	**34**	**1.5**	**0.2**	n.d.	**0.06**	**1.2**	n.d.
8	**10**	**15**	**5.7**	**0.9**	**2.5**	**0.2**	**1.1**	**0.05**

[a] For the non-A_L-type phase-solubility diagrams, initial slopes *m* are taken. Values are given in italics. [b] n.d. = solubility enhancement of guest was not detectable.

To gain further insight into the host–guest stoichiometries of the complexes, fluorescence spectroscopy was employed, because complexation of two chromophores within a CD cavity is known to cause excimer formation, thereby leading to large Stokes shifts. Excimer formation was already observed for CD complexes of NAP,[18] STI,[19] ANT,[20] and pyrene.[21]

The fluorescence spectra of the inclusion compounds of the aromatic guests in γ-CD derivative **1** showed a single emission band in each case with pronounced Stokes shifts of $\Delta\lambda = 71$ to 124 nm (these are listed in Table 4, and detailed spectra are collected in the Supporting Information). For comparison, the corresponding heptakis[6-deoxy-6-(2-aminoethylsulfanyl)]-β-CD (β-**1**),[2c,9] which only accommodates one single guest, showed much smaller Stokes shifts of $\Delta\lambda =$ 26 to 83 nm, typical for dilute solutions of the fluorophores in organic solvents. Consequently, the large extra Stokes shifts $\Delta\Delta\lambda$, listed in Table 4, strongly support our hypothesis of two aromatic guests being included in the large cavity of the γ-CD derivative **1**. Only the $\Delta\Delta\lambda$ value for guest TET (15 nm) was significantly less than that of the other guests. Therefore 1:2 CD–guest complexes are less likely to have been formed in this case.

Table 4. Absorption (λ_{ab}) and emission (λ_{em}) maxima [nm], and Stokes shift values ($\Delta\lambda$) [nm] of aromatic guests in water in the presence of β-CD derivative β-**1** and γ-CD derivative **1** at 298 K.

Guest	β-**1**			**1**			$\Delta\Delta\lambda$[a]
	λ_{ab}	λ_{em}	$\Delta\lambda$	λ_{ab}	λ_{em}	$\Delta\lambda$	
NAP	300	325	25	337	424	87	62
NCA	343	374	31	340	412	72	41
AZU	365	377	12	353	424	71	59
STI	310	356	46	351	428	77	31
ACE	354	437	83	284	408	124	41
ANT	361	406	45	294	368	74	29
PHE	357	368	11	290	367	77	66
TET	367	424	57	360	432	72	15

[a] $\Delta\Delta\lambda$ is equal to the excess Stokes shift values of guests complexed in γ-CD derivatives **1** compared to those complexed in β-**1**.

Typical absorption and emission spectra of STI in the presence of CD derivatives in aqueous solution are shown as examples in Figure 2. A small Stokes shift ($\Delta\lambda =$ 46 nm) was found for STI complexed in β-**1**, whereas a large Stokes shift ($\Delta\lambda = 77$ nm) was observed for STI in γ-CD derivative **1**. Both emission bands were narrow and monomodal, thus demonstrating that only one species of stilbene complex existed in each case, namely, the 1:1 and the 1:2 complexes, respectively. This finding was in contrast to the fluorescence spectra obtained for the complex of naphthalene in native β-CD, for which a broad bimodal fluorescence was found.[18] The formation of a 2:2 complex was discussed for the NAP-β-CD system. This model appeared implausible for the

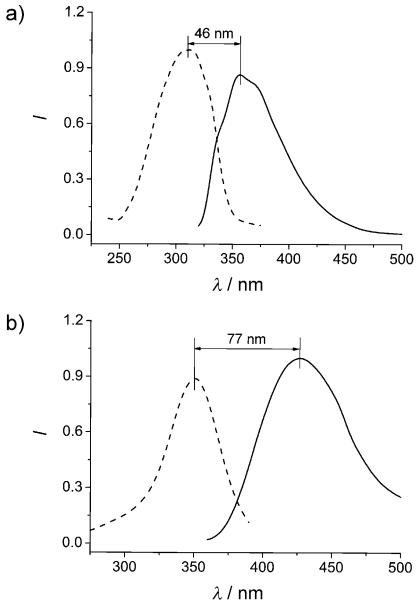

Figure 2. Absorption (dashed line) and emission (solid line) spectra of the inclusion system of a) STI with β-**1** and b) CD **1** in aqueous solution.

complexes of aromatic guests in γ-CD derivatives described here, because narrow excimer emission bands were already observed for very low concentrations of γ-CD derivative **1**. For a further clarification of the stoichiometries of complexes of γ-CD derivatives **1**–**8**, molecular packing was investigated by molecular modeling studies.

Table 5. In-plane areas A and maximum cross-sectional areas A_{max} (in Å^2) in direction of the long axis and short axis of the molecule of the aromatic guest molecules.

	Guest							
	NAP	NCA	AZU	STI	ACE	ANT	PHE	TET
A_{max} long axis	31.4	62.0	40.2	82.3	31.4	64.3	64.3	100.0
A_{max} short axis	20.0	23.4	22.7	19.9	28.5	21.6	24.1	21.6
A in plane	55.0	65.0	55.5	78.4	61.7	62.8	72.0	90.3

Molecular Modeling

Although the modification of γ-CD on the primary rim with side arms changes the height of γ-CD, the internal diameter d of the γ-CD should remain unaffected. According to this view, γ-CD was selected as a simple model host throughout the theoretical calculations. Quantum mechanical calculations were employed to obtain the inner surface (electron density map) of the γ-CD cavity. The cross-sectional area A of the γ-CD cavity was obtained by analysis of the electron density map of γ-CD with the program MolShape,[22] which was already useful for prediction of stoichiometries of polyrotaxanes.[2b] Thus, the corresponding profile of the inner width d of the γ-CD cavity along the C_8 axis was obtained.

The maximum inner diameter (cross-sectional area) at the secondary rim of γ-CD was determined to be $d_{max}=10.3$ Å ($A_{max}=83.5$ Å^2). The minimum internal diameter $d_{min}=8.0$ Å ($A_{min}=50.6$ Å^2), situated approximately at hydrogen H-5 of the γ-CD cavity was found, which was in good accordance with the results of both experimental measurements and other theoretical calculations.[1c,22,23] Similarly, the maximum cross-sectional areas A_{max} of the aromatic guests were calculated, both in direction of the short and the long axis of the molecule, and also the areas A in the plane of the molecules, summarized in Table 5. The dimeric aromatic guest can fit principally in three possible orientations, with the long axis, the short axis, and both axes perpendicular to the C_8 axis in the γ-CD cavity, depicted in Scheme 3. From these calculations it became clear that all guests can be accommodated in the complete γ-CD cavity as dimers with their short axis oriented perpendicular to the C_8 axis (Scheme 3b), because twice the corresponding cross-sectional area A_{max} of the guest is less or equal to the minimum cross-sectional area $A_{min}=50.6$ Å^2 of the host. The predominance of this orientation is in accordance with other experimental results.[11c–e,k] The other orientations are not possible because of geometrical constraints. The smaller dimensions of the β-CD cavity, $A_{min}=34.6$ Å^2 and $A_{max}=60.4$ Å^2 explain why the NAP dimer can only protrude partially in it, which leads to the formation of 2:2 complexes, necessary for a complete coverage of the dimer.[18]

Quantum mechanical calculations of the structures and interaction energies ΔE of the aromatic dimers were performed using the Gaussian 03 software package.[24] Former experimental and theoretical investigations on the aromatic dimers indicated that the dimers with the largest overlapping areas generally would have the most negative values of intermolecular interaction energy. Accordingly, in this work, two starting orientations of the aromatic dimers were considered (i.e., the parallel ↑↑ and antiparallel ↑↓ orientations). Given that dispersion forces are known to play an important role in the energetics of aromatic dimers, it is imperative that the calculation of the energies has to be made at the level of second-order Møller–Plesset perturbation theory (MP2).[25] The aromatic dimers were fully optimized at the MP2/6-31G* level without any symmetry restriction. The resulting interaction energies ΔE, the center of mass distances d, and the maximum cross-sectional areas A_{max} in the direction of the short axis are collected in Table 6. The interaction energy ΔE became more negative with increasing size of the molecule, and was in good accordance with published data.[25,26] Remarkable differences in ΔE values of the aromatic dimers, which possess two stable orientations, were clearly observed from Table 6. For instance, the ΔE value of NCA dimer with antiparallel orientation was found to be significantly more negative than that of the dimer with parallel orientation. This result can be attributed to the ad-

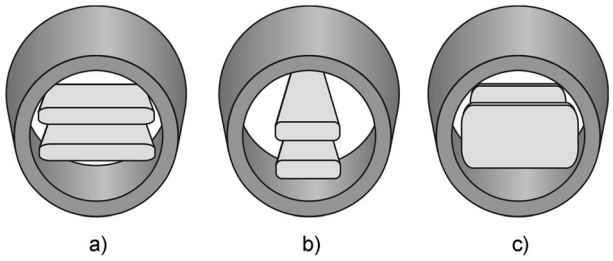

Scheme 3. Schematic drawing depicting the top view of 1:2 γ-CD complexes for three possible orientations: a) long axis, b) short axis, and c) both axes perpendicular to the C_8 axis of γ-CD.

Table 6. The intermolecular interaction energies (ΔE) and the distances d of the mass centers of the two guests within the dimer, and the calculated maximal cross-sectional areas (A_{max}) of the optimized aromatic dimers.

Dimer[a]	ΔE [kJ mol^{-1}]	d [Å]	A_{max} [Å^2]
NAP	−17.8	3.64	44.8
NCA (dimer ↑↓)	−18.0	3.69	52.3
AZU (dimer ↑↑)	−21.8	3.60	52.0
AZU (dimer ↑↓)	−34.6	3.29	51.0
STI	−22.3	3.91	57.1
ACE (dimer ↑↑)	−20.5	3.54	53.1
ACE (dimer ↑↓)	−29.2	3.18	52.0
ANT	−31.0	3.65	49.6
PHE (dimer ↑↑)	−27.6	3.86	56.8
PHE (dimer ↑↓)	−21.9	3.85	66.7

[a] For the NCA dimer ↑↑, a T-shaped orientation was obtained after optimization.

CHEMISTRY
AN ASIAN JOURNAL

ditional dipole–dipole interaction between the two monomers in the antiparallel orientation. Similar phenomena also occurred for the aromatic dimers of AZU and ACE. The corresponding distances *d* between two monomers in these parallel-configured dimers were found to be remarkably larger than those of the monomers with antiparallel orientation. Contrarily, the interaction energy of the parallel-oriented dimer of PHE was more negative than the one of the antiparallel dimer. It appeared reasonable that the relatively poor overlap between two PHE molecules in the antiparallel dimer caused this result.[27]

It has to be noted that the cross-sectional areas A_{max} derived from the calculated structures of the dimers are larger than twice of the calculated cross-sectional area of the corresponding monomer. But these more realistic A_{max} values from Table 6 are still small enough to fit in the γ-CD cavity.

The packing of AZU dimer in the γ-CD cavity is provided as an example in Figure 3. This dimer fits well into the cavity of γ-CD without steric hindrance. As can be seen, both orientations within the dimer, parallel (Figure 3b) and antiparallel (Figure 3c), were perfectly accommodated into the cavity of γ-CD. The antiparallel orientation of AZU appears to be more probable because of its more negative ΔE value. Consequently, taking together all facts such as the very good space filling of the γ-CD cavity, the sufficiently large negative values of ΔE, and the observed large Stokes shifts, the formation of 1:2 host–guest complexes became evident. After determination of the stoichiometry, binding constants and binding free energies could be finally calculated.

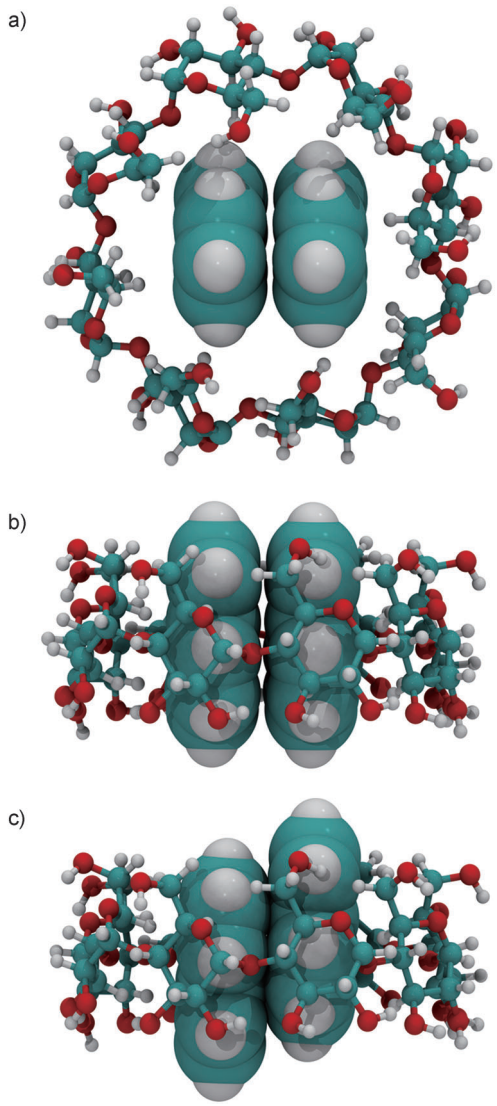

Figure 3. Schematic drawing depicting the AZU dimer in γ-CD: a) top view, b) side view ↑↑ orientation, and c) side view ↑↓ orientation.

Binding Free Energy

Binding constants *K* and binding free energies ΔG were calculated from the slope *m* of the solubility isotherm and the solubilities of the free guests in water according to Equations (7) and (8), respectively (see the Experimental Section below). The calculated ΔG values of the aromatic guests with γ-CD or γ-CD derivatives are summarized in Table 7. As discussed above, as TET is less likely to form an 1:2 inclusion complex with γ-CD or γ-CD derivatives, it was excluded from the discussion. Pronounced differences between the ΔG values were observed for the various guests. Guests AZU, ANT, and PHE showed more negative ΔG values (around $-55\,kJ\,mol^{-1}$) than NAP and NCA (around $-35\,kJ\,mol^{-1}$), which was in good correlation with the more negative interaction energies ΔE of AZU, ANT, and PHE dimers (around $-31\,kJ\,mol^{-1}$) relative to NAP and NCA (around $-19\,kJ\,mol^{-1}$). This means that the interaction energy of the dimer provides a major contribution to binding free energy. Despite its strongly negative ΔE value, ACE only shows a moderate ΔG value, which might be due to its large cross-sectional area along its short axis, which might lead to a very tight fit within the γ-CD cavity. In our previous work, we found that a loose fit of a guest in a CD cavity leads to a higher binding constant than a tight fit, possibly due to entropic effects.[22] These entropic effects would also explain why the slim guest STI shows a strongly negative ΔG value, whereas its ΔE value is only moderate.

Conclusion

In the present work, we have synthesized and characterized a series of octasubstituted γ-CD derivatives with various neutral or ionic side arms bound through thioether linkages to the CD scaffold. It was found that these γ-CD derivatives showed much higher solubilization abilities for aromatic guests than native CDs or other frequently used derivatives such as hydroxypropyl-β-CD. The existence of 1:2 host–guest complexes was confirmed from the phase-solubility data, the excimer emissions, as well as theoretical investigations. The ΔG values of the CD–guest complexes obtained from the solubility data are strongly negative because the interaction energy between the included guests makes the

Table 7. Binding free energies (ΔG) [kJ mol^{-1}] for the complexation of aromatic guests in γ-CD and γ-CD derivatives at 298 K.

Host	Guest[a]						
	NAP	NCA	AZU	STI	ACE	ANT	PHE
γ-CD	-	*−31.0*	**−51.6**	**−48.9**	**–**	**−50.3**	**−52.1**
1	**−38.9**	–	**−59.3**	**−58.5**	**−40.9**	**−59.1**	**−59.2**
2	**−32.8**	**−43.9**	**−58.3**	**−54.1**	**−40.7**	**−56.4**	**−58.4**
3	**−38.3**	**−37.4**	**−60.7**	**−56.0**	**−43.2**	**−56.1**	**−59.6**
4	**−34.5**	**−41.0**	**−56.3**	**−54.3**	**−40.6**	**−54.4**	**−58.7**
5	*−35.8*	**−35.5**	**−58.5**	**−54.8**	**−37.6**	**−54.6**	*−57.7*
6	**−36.8**	**−37.3**	**−59.9**	**−55.9**	**−42.4**	**−56.0**	**−60.4**
7	*−38.2*	**−35.9**	**−54.6**	**−53.4**	**–**	**−52.0**	**−53.0**
8	**−35.2**	**−33.7**	**−58.0**	**−57.9**	**−36.8**	**−56.4**	**−58.6**

[a] ΔG values given in italics were calculated on the basis of the initial slope m of the phase-solubility diagrams.

main contribution to the driving force of complex formation.

These γ-CD derivatives are good candidates for molecular reaction vessels for photodimerization reactions of native polycyclic aromatic molecules in aqueous solution. The significantly enhanced solubilities of the aromatic guests in water would allow photodimerization of these guests under homogenous conditions for the first time. The kinetics as well as the stereo- and regioselectivities[28] of the photodimerizations of these guests mediated by the γ-CD derivatives will be investigated in our future works.

Experimental Section

General

Unless otherwise stated, all chemicals were used as received. Corresponding thiol compounds for the synthesis of γ-CD derivatives **1**–**7** were purchased from Sigma Aldrich. The thiol compound for the synthesis of **8** was synthesized and purified according to a published procedure.[29]

Solvents were dried as follows: DMF over P_2O_5 and distilled; pyridine over KOH; and methanol distilled from iodine and magnesium turnings immediately before use.[30] α-, β-, and γ-CD were dried in vacuo at 100 °C overnight. γ-CD derivatives were purified by nanofiltration (molecular weight cutoff: 1000 Da).

Teflon syringe filters (0.22 μm) from Roth, Karlsruhe, Germany were used to remove insoluble material before UV/Vis and fluorescence measurements. Thin-layer chromatography (TLC) was performed on aluminum sheets coated with silica gel (F254) and developed by charring with 5% H_2SO_4 in ethanol. Electrospray ionization mass spectrometric (ESI-MS) analysis was performed with an ESI single-quadrupole mass spectrometer (micromass ZQ 4000, Waters) from solutions in water. The following settings were used: capillary voltage 3.80 kV, cone voltage 20 V, extractor voltage 5 V. UV/Vis spectra of aqueous samples were performed with a Perkin–Elmer Lambda 2 spectrometer (λ: 200–600 nm), using quartz cells with a 1 cm or 1 mm optical path at 298 K. Fluorescence spectra were recorded with a JASCO spectrophotometer using quartz cells of 10.0 mm path at 298 K. All NMR spectra were recorded with a Bruker 400 MHz NMR spectrometer at 298 K using the solvent peaks as internal references. Coupling constants (J) were measured in Hz. The signals are described as follows: s (singlet), d (doublet), t (triplet), and m (multiplet).

*Octakis(6-deoxyiodo)-γ-CD (**9**)*

As shown in Scheme 2, Ph_3P (104.92 g, 400 mmol) was dissolved in anhydrous DMF (320 mL). Under an N_2 atmosphere, I_2 (104.06 g, 410 mmol) was added over 15 min at 0 °C. Dry γ-CD (25.94 g, 20 mmol) was then added. The solution was concentrated in vacuo to half volume after stirring at 70 °C for 24 h. NaOMe in MeOH (3 M, 160 mL) was then added under cooling and stirred for 30 min at RT. The thick reaction mixture was poured into methanol (2.5 L) under vigorous stirring to form a brownish precipitate, which was filtered, washed afterwards with MeOH (0.5 L), and dried. The brown solid was dissolved in dry pyridine (130 mL). Ac_2O (130 mL) was added, and the resulting solution was stirred for 2 d at room temperature. Methanol (70 mL) was added and stirred for 1 h to quench the reaction. Column chromatography on silica gel and ethyl acetate (EtOAc)/*n*-hexane (4:1) as an eluent gave a pale yellow solid (R_f = 0.2–0.3). The raw product was then suspended in anhydrous MeOH (200 mL) that contained NaOMe (0.50 g) for 4 d. Compound **9** was recovered as a white powder after suction filtration. Yield: 28.54 g (13.1 mmol, 66%); ^{1}H NMR (400 MHz, [D$_6$]DMSO): δ = 5.96–5.97 (d, J = 2.8 Hz, 8H; OH-2), 5.95 (s, 8H; OH-3), 5.02–5.03 (d, J = 3.6 Hz, 8H; H-1), 3.79–3.82 (d, J = 9.2 Hz, 8H; H-3), 3.57–3.67 (m, 16H; H-6a,b), 3.44–3.55 (m, 16H; H-4,5), 3.25–3.30 ppm (t, J = 9.0 Hz, 8H; H-2); ^{13}C NMR (100 MHz, [D$_6$]DMSO): δ = 9.25, 71.08, 71.80, 72.37, 85.24, 101.93 ppm.

General Procedure for the Synthesis of Neutral Octakis-6-deoxy-γ-CD

A procedure identical to that described previously was utilized (Scheme 2).[2a] Triethylamine (3.98 mL, 28.57 mmol) and the corresponding thiol compound (28.57 mmol) were added with stirring to a solution of **9** (3.11 g, 1.43 mmol) in DMF (15 mL). After stirring for 3 d at 60 °C under N_2, the crude product was diluted with sufficient amount of appropriate organic solvents. The resulting precipitate was filtered off, washed, dried in vacuo, and then purified by ultrafiltration.

General Procedure for the Synthesis of Ionic Octakis-6-deoxy-γ-CD

Triethylamine (3.98 mL, 28.57 mmol) and the corresponding methyl ester of the thiol compound (28.57 mmol) were added to a solution of compound **9** (3.11 g, 1.43 mmol) in DMF (15 mL). After stirring for 3 d at 60 °C under N_2 atmosphere, the reaction mixture was diluted with sufficient amount of appropriate organic solvents. The resulting precipitate was collected, then stirred in NaOH (1 M) for 18 h, and then further purified by ultrafiltration.

*Octakis[6-deoxy-6-(2-aminoethylsulfanyl)]-γ-CD (**1**)*

Compound **1** was synthesized according to the general procedure. The crude product was precipitated in acetone, dissolved in water, ultrafiltered, and lyophilized. Yield: 1.80 g (71%), white solid; ^{1}H NMR (400 MHz, D_2O, 25 °C): δ = 5.17–5.18 (d, J = 3.6 Hz, 8H; H-1), 3.88–3.97 (m, 16H; H-3,5), 3.65–3.69 (dd, J = 10.0 Hz, 8H; H-2), 3.52–3.57 (t, J = 9.4 Hz, 8H; H-4), 2.91–3.28 (m, 16H; H-6a,6b), 2.80–2.86 ppm (dd, J = 20.0 Hz, 32H; H-7,8); ^{13}C NMR (100 MHz, D_2O, 25 °C): δ = 35.33, 39.97, 64.56, 71.65, 72.70, 83.32, 100.01 ppm; MS (3.80 kV, ESI, water): m/z (%): 1769.84 (20) $[M+H]^+$, 884.40 (79) $[M+2H]^{2+}$, 589.57 (100) $[M+3H]^{3+}$.

*Octakis[6-deoxy-6-(2-sulfanyl acetic acid)]-γ-CD (**2**)*

Compound **2** was synthesized according to the general procedure. The crude product was precipitated in ethanol, stirred in 1 M NaOH for 18 h, ultrafiltered, and lyophilized. Yield: 1.82 g (62%), white solid; ^{1}H NMR (400 MHz, D_2O, 25 °C): δ = 5.13–5.14 (d, J = 3.6 Hz, 8H; H-1), 4.01–4.05 (m, 8H; H-5), 3.87–3.92 (t, J = 9.6 Hz, 8H; H-3), 3.66–3.70 (t, J = 9.4 Hz, 8H; H-2), 3.59–3.62 (dd, J = 10.0 Hz, 8H; H-4), 3.30–3.38 (m, 16H; H-7), 2.90–3.12 ppm (m, 16H; H-6a,6b); ^{13}C NMR (100 MHz, D_2O, 25 °C): δ = 33.73, 38.60, 71.37, 72.31, 72.61, 82.45, 101.19, 177.71 ppm; MS (3.80 kV, ESI, water): m/z (%): 1912.60 (25) $[M+Na]^+$, 967.84 (100) $[M+2Na]^{2+}$.

*Octakis[6-deoxy-6-(2-sulfanylethanesulfonic acid)]-γ-CD (**3**)*

Compound **9** (3.11 g, 1.43 mmol), sodium 2-mercaptoethanesulfonate (4.60 g, 28.00 mmol), and triethylamine (3.98 mL, 28.57 mmol) were dissolved in DMSO (25 mL). After stirring for 3 d at 60 °C under N_2, the product was precipitated in acetone, dissolved in water, ultrafiltered, and

lyophilized. Yield: 3.25 g (92%), white solid; ^{1}H NMR (400 MHz, D_2O, 25°C): δ=5.14–5.15 (d, J=3.6 Hz, 8H; H-1), 4.00–4.05 (m, 8H; H-5), 3.88–3.93 (t, J=9.6 Hz, 8H; H-3), 3.58–3.62 (m, 16H; H-2,4), 3.11–3.21 (m, 24H; H-6a,7), 2.91–2.99 ppm (m, 24H; H-6b,8); ^{13}C NMR (100 MHz, D_2O, 25°C): δ=27.27, 33.27, 51.37, 71.32, 72.26, 72.68, 100.01, 100.96 ppm; MS (3.80 kV, ESI, water): m/z (%): 1257.66 (100) $[M+2Na]^{2+}$.

*Octakis[6-deoxy-6-(2-sulfanylpropanoic acid)]-γ-CD (**4**)*

Compound **4** was synthesized according to the general procedure. The crude product was precipitated in 2-propanol, stirred in 1 M NaOH for 18 h, ultrafiltered, and lyophilized. Yield: 1.27 g (41%), white solid; ^{1}H NMR (400 MHz, D_2O, 25°C): δ=5.21–5.22 (m, 8H; H-1), 3.98–4.09 (m, 16H; H-3,5), 3.50–3.76 (m, 24H; H-2,4,7), 3.11–3.22 (m, 8H; H-6a), 2.96–2.99 (m, 8H; H-6b), 1.43–1.45 ppm (d, J=7.2 Hz, 24H; H-8). MS (3.80 kV, ESI, water): m/z (%): 2025.30 (65) $[M+Na]^+$, 1024.57 (100) $[M+2Na]^{2+}$.

*Octakis[6-deoxy-6-(3-sulfanylpropane-1,2-diol)]-γ-CD (**5**)*

Compound **5** was synthesized according to the general procedure. The crude product was precipitated in ethanol, dissolved in water, ultrafiltered, and lyophilized. Yield: 2.44 g (85%), white solid; ^{1}H NMR (400 MHz, D_2O, 25°C): δ=5.18–5.19 (d, J=3.2 Hz, 8H; H-1), 4.00–4.05 (t, J=8.4 Hz, 8H; H-5), 3.90–3.95 (m, 16H; H-3,8), 3.57–3.72 (m, 32H; H-2,4,7), 3.25–3.28 (d, J=12.8 Hz, 8H; H-6a), 3.00–3.03 (m, 8H; H-6b), 2.74–2.92 ppm (m, 16H; H-9); ^{13}C NMR (100 MHz, D_2O, 25°C): δ= 34.00, 35.93, 64.54, 71.04, 71.45, 72.26, 72.70, 83.32, 101.33 ppm; MS (3.80 kV, ESI, water): m/z (%): 2039.63 (29) $[M+Na]^+$, 1030.89 (100) $[M+2Na]^{2+}$.

*Octakis[6-deoxy-6-(3-sulfanylpropanoic acid)]-γ-CD (**6**)*

Compound **6** was synthesized according to the general procedure. The crude product was precipitated in ethanol, stirred in 1 M NaOH for 18 h, ultrafiltered, and lyophilized. Yield: 2.55 g (82%), white solid; ^{1}H NMR (400 MHz, D_2O, 25°C): δ=5.15–5.14 (d, J=3.2 Hz, 8H; H-1), 4.01–4.04 (t, J=8.4 Hz, 8H; H-5), 3.89–3.93 (t, J=9.4 Hz, 8H; H-3), 3.58–3.64 (m, 16H; H-2,4), 2.93–3.11 (m, 16H; H-6a,b), 2.80–2.84 (t, J=7.4 Hz, 16H; H-7), 2.43–2.47 ppm (m, 16H; H-8); ^{13}C NMR (100 MHz, D_2O, 25°C): δ=29.54, 33.34, 37.75, 64.56, 71.29, 73.01, 83.56, 100.01, 180.73 ppm; MS (3.80 kV, ESI, water): m/z (%): 2023.63 (20) $[M+Na]^+$, 1023.89 (100) $[M+2Na]^{2+}$.

*Octakis[6-deoxy-6-(2-hydroxyethylsulfanyl)]-γ-CD (**7**)*

Compound **7** was synthesized according to the general procedure. The reaction mixture was poured into ethanol. The formed precipitate was collected by suction filtration, recrystallized in cold water, and dried to give **7** (yield: 2.19 g, 86%) as colorless needles. ^{1}H NMR (400 MHz, [D_6]DMSO, 25°C): δ=5.91 (s, 16H; OH-2,3), 4.92–4.93 (d, J=3.6 Hz, 8H; H-1), 4.70–4.72 (t, J=5.4 Hz, 8H; OH-9), 3.72–3.76 (m, 8H; H-5), 3.50–3.59 (m, 24H; H-2,3,4), 3.32–3.41 (m, 16H; H-7), 2.79–3.09 (m, 16H; H-6a,b), 2.62–2.67 ppm (m, 16H; H-8); MS (3.80 kV, ESI, water): m/z (%): 1799.52 (65) $[M+Na]^+$, 911.37 (100) $[M+2Na]^{2+}$, 1775.88 (100) $[M-H]^-$.

*Octakis[6-deoxy-6-(10-sulfanyl-2,5,8-trioxodecane)]-γ-CD (**8**)*

Compound **8** was synthesized according to the general procedure. The crude product was precipitated in diethyl ether, ultrafiltered, and lyophilized. Yield: 3.02 g (81%), white solid; ^{1}H NMR (400 MHz, D_2O, 25°C): δ=5.03–5.04 (d, J=3.6 Hz, 8H; H-1), 3.71–3.80 (m, 16H; H-3,5), 3.62–3.66 (m, 16H; H-2,4), 3.40–3.59 (m, 80H; H-10), 3.29 (s, 24H; H-9), 2.80–3.25 ppm (m, 32H; H-6,7,8); MS (3.80 kV, ESI, water): m/z (%): 1297.63 (35) $[M+2H]^{2+}$, 2593.48 (100) $[M-H]^-$.

Phase-Solubility Investigations

Since the effective polarity of the CD cavity was proven to be similar to that of ethanol,[10c,31] the molar extinction coefficients (ε) of NAP, NCA, AZU, ACE, ANT, and PHE were measured in ethanol. However, due to their low solubilities in ethanol, the ε values of STI and TET were measured in 1,4-dioxane and dichloromethane, respectively. The observed ε values of the aromatic guests at their absorption maxima (λ) are summarized in Table 8.

Table 8. Molar extinction coefficients (ε) [L mol^{-1} cm^{-1}] of guests at the absorption maxima (λ) [nm].

	Guest							
	NAP	NCA	STI	AZU	ACE	ANT	PHE	TET
λ	275	280	310	339	322	356	293	277
ε	5590	6950	18570	4370	9090	7350	11710	100700

Solubility measurements of the guests in the presence of native CDs and γ-CD derivatives in water were carried out according to the method proposed by Higuchi and Connors.[14] In glass vials that contained excess amounts of guest molecules, aqueous solutions of native CDs or γ-CD derivatives (concentration of CD: 1.0, 2.0, 3.0, 4.0, and 6.0 mM) were added. The vials were sealed, protected from light, and magnetically stirred at room temperature. After 72 h, the solid residues were removed by filtration with syringe filter. According to Lambert–Beer's law, the concentrations of guests in pure water and in CDs solutions were determined from UV/Vis extinctions at the absorption maxima.

Determination of Binding Free Energy

The increase in water solubility of a guest molecule is due to the intermolecular interactions between the guest molecule and CD to form soluble complexes.[5b,14b,32] The binding constants ($K_{1:n}$) for the formation of a 1:n inclusion complex between CD and guest molecule can be expressed as Equation (1):

$$K_{1:n} = \frac{[HG]}{[H] \cdot [G]^n} \quad (1)$$

in which n is the guest–host ratio, and [H], [G], and [HG] are the concentrations of the free CD, the free guest, and the corresponding inclusion complex, respectively.

Assuming that the concentration of the free guest in CD solution is equal to that in pure water $[G]_0$, the following equations can be obtained [Eqs. (2), (3), and (4)]:[33]

$$[G] = [G]_0 \quad (2)$$

$$[HG] = (1/n)([G]_t - [G]_0) \quad (3)$$

$$[H] = [H]_t - [HG] \quad (4)$$

in which $[G]_0$ is the equilibrium solubility of guest in pure water, and $[H]_t$ and $[G]_t$ correspond to the total concentrations of CD and guest, respectively.

Substituting Equations (2–4) into Equation (1) affords Equation (5):

$$K_{1:n} = \frac{[G]_t - [G]_0}{[G]_0^n \cdot ([H]_t - ([G]_t - [G]_0)/n)} \quad (5)$$

The slope (m) of the dependence line is represented by Equation (6) as follows:

$$m = \frac{[G]_t - [G]_0}{[H]_t} \quad (6)$$

A plot of $[G]_t$ against $[H]_t$ yields a straight line. Thus, the binding constant between CD and guest can be calculated from the phase diagrams using Equation (7):

$$K_{1:n} = \frac{m}{[G]_0^n \cdot (n-m)} \quad (7)$$

The binding free energy (ΔG) is calculated according to Equation (8):

$$\Delta G = -RT \ln K \quad (8)$$

Molecular Modeling

All quantum mechanical calculations were carried out with the Gaussian 03 software package.[24] The initial geometries of the aromatic guests were built up from their respective crystal structures[34] and then fully optimized without any symmetrical restrictions at the MP2/6-31G* level. The input structures of β- and γ-CD were taken from existing crystallographic data[23,35] and fully optimized by the PM3 method.[36] The glycosidic oxygen atoms of CDs were placed onto the *xy* plane, and the center of the glycosidic oxygen atoms was designated as the origin of the Cartesian coordinate system. The secondary OH rim of CDs was placed pointing toward the positive *z* axis. The rendering was performed with VMD 1.8.7.[37]

Cross-Sectional Area

The electron density function was transformed into a discrete cubic electron density by using the program Cubegen from Gaussian 03.[24] The cross-sectional diameters and the cross-sectional areas of CD and the guest molecules were then calculated from the cubic electron densities by the program MolShape.[22] An electron density cutoff value of 0.002 au was chosen to define the surface of the molecule.[22]

Aromatic Dimer

The aromatic dimers were built up by combining two optimized monomers together, and then used as initial guesses for full geometry optimizations of the gas-phase dimers at the MP2/6-31G* level of theory. The planes of two monomers with a center-to-center distance of 3.5 Å were parallel with each other. In the present case, the geometries of the orientational isomers were fully optimized without any symmetry restriction. Interaction energies (ΔE) that corresponded to the optimized aromatic dimers (parallel ↑↑ and antiparallel ↑↓ orientation) were evaluated by $\Delta E = E_{dimer} - 2E_{monomer}$ at the MP2/6-31G* level, in which E_{dimer} and $E_{monomer}$ are energies of the aromatic dimer and the monomer, respectively. ΔE values were corrected for basis set superposition error (BSSE) by means of the counterpoise correction of Boys and Bernardi.[38]

Acknowledgements

We gratefully thank the technical support from Annegret Engelke and Mathias Grosser. We would also like to express our appreciation to Dagmar Auerbach for her assistance in fluorescence spectroscopy measurements and Yi Dong and Michael Springborg from Saarland University for helpful discussions concerning molecular modeling. Financial support from Saarland University and China Scholarship Council is gratefully acknowledged.

[1] a) G. Wenz, *Angew. Chem.* **1994**, *106*, 851–870; *Angew. Chem. Int. Ed. Engl.* **1994**, *33*, 803–822; b) G. Wenz, *J. Polym. Sci. Part A* **2009**, *47*, 6333–6341; c) J. Szejtli, *Chem. Rev.* **1998**, *98*, 1743–1753.

[2] a) A. Steffen, C. Thiele, S. Tietze, C. Strassnig, A. Kamper, T. Lengauer, G. Wenz, J. Apostolakis, *Chem. Eur. J.* **2007**, *13*, 6801–6809; b) G. Wenz, B. H. Han, A. Müller, *Chem. Rev.* **2006**, *106*, 782–817; c) G. Wenz, C. Strassnig, C. Thiele, A. Engelke, B. Morgenstern, K. Hegetschweiler, *Chem. Eur. J.* **2008**, *14*, 7202–7211.

[3] a) K. Uekama, F. Hirayama, T. Irie, *Chem. Rev.* **1998**, *98*, 2045–2076; b) A. R. Hedges, *Chem. Rev.* **1998**, *98*, 2035–2044; c) T. Loftsson, M. Brewster, *J. Pharm. Sci.* **1996**, *85*, 1017–1025; d) K. Kano, Y. Ishida, *Angew. Chem.* **2007**, *119*, 741–744; *Angew. Chem. Int. Ed.* **2007**, *46*, 727–730.

[4] a) I. Beà, M. G. Gotsev, P. M. Ivanov, C. Jaime, P. A. Kollman, *J. Org. Chem.* **2006**, *71*, 2056–2063; b) Y. Liu, B.-H. Han, H.-Y. Zhang, *Curr. Org. Chem.* **2004**, *8*, 35–46; c) K. Kano, Y. Ishida, *Chem. Asian J.* **2008**, *3*, 678–686.

[5] a) S. Filippone, F. Heimann, A. Rassat, *Chem. Commun.* **2002**, 1508–1509; b) T. Loftsson, D. Hreinsdottir, M. Masson, *Int. J. Pharm.* **2005**, *302*, 18–28.

[6] T. Loftsson, A. Magnusdottir, M. Masson, J. F. Sigurjonsdottir, *J. Pharm. Sci.* **2002**, *91*, 2307–2316.

[7] a) G. Wenz, T. Hofler, *Carbohydr. Res.* **1999**, *322*, 153–165; b) J. Pitha, J. Milecki, H. Fales, L. Pannell, K. Uekama, *Int. J. Pharm.* **1986**, *29*, 73–82.

[8] V. Zia, R. A. Rajewski, V. J. Stella, *Pharm. Res.* **2001**, *18*, 667–673.

[9] K. Kano, Y. Ishida, K. Kitagawa, M. Yasuda, M. Watanabe, *Chem. Asian J.* **2007**, *2*, 1305–1313.

[10] a) M. Lubomska, P. Gierycz, M. Rogalski, *Fluid Phase Equilib.* **2005**, *238*, 39–44; b) X. Wang, M. L. Brusseau, *Environ. Sci. Technol.* **1995**, *29*, 2346–2351; c) X. Wang, M. L. Brusseau, *Environ. Sci. Technol.* **1993**, *27*, 2821–2825.

[11] a) K. Takahashi, *Chem. Rev.* **1998**, *98*, 2013–2033; b) X. Wu, L. Lei, L. Wu, G. Liao, L. Luo, X. Shan, L. Zhang, C. Tung, *Tetrahedron* **2007**, *63*, 3133–3137; c) L. Luo, G. H. Liao, X. L. Wu, L. Lei, C. H. Tung, L. Z. Wu, *J. Org. Chem.* **2009**, *74*, 3506–3515; d) C. Yang, A. Nakamura, T. Wada, Y. Inoue, *Org. Lett.* **2006**, *8*, 3005–3008; e) A. Nakamura, Y. Inoue, *J. Am. Chem. Soc.* **2005**, *127*, 5338–5339; f) S. Karthikeyan, V. Ramamurthy, *Tetrahedron Lett.* **2005**, *46*, 4495–4498; g) N. Haga, H. Takayanagi, K. Tokumaru, *J. Org. Chem.* **1997**, *62*, 3734–3743; h) F. D. Lewis, S. V. Barancyk, E. L. Burch, *J. Phys. Chem.* **1992**, *96*, 2548–2553; i) K. Wei, R. Livingston, *Photochem. Photobiol.* **1967**, *6*, 229–232; j) J. Reichwagen, H. Hopf, A. Del Guerzo, J. Desvergne, H. Bouas-Laurent, *Org. Lett.* **2004**, *6*, 1899–1902; k) W. Herrmann, S. Wehrle, G. Wenz, *Chem. Commun.* **1997**, 1709–1710.

[12] A. Nakamura, Y. Inoue, *J. Am. Chem. Soc.* **2003**, *125*, 966–972.

[13] P. R. Ashton, R. Koniger, J. F. Stoddart, D. Alker, V. D. Harding, *J. Org. Chem.* **1996**, *61*, 903–908.

[14] a) R. Singh, H. H. Tonnesen, S. B. Vogensen, T. Loftsson, M. Masson, *J. Inclusion Phenom. Macrocyclic Chem.* **2010**, *66*, 335–348; b) T. Higuchi, K. Connors, *Adv. Anal. Chem. Instrum.* **1965**, *4*, 117–212; c) T. Higuchi, H. Kristiansen, *J. Pharm. Sci.* **1970**, *59*, 1601–1608.

[15] a) A. Chauhan, N. Jain, P. Diwan, A. Khopade, *J. Drug Targeting* **2004**, *12*, 575–583; b) S. Tenjarla, P. Puranajoti, R. Kasina, T. Mandal, *J. Pharm. Sci.* **1998**, *87*, 425–429.

[16] H. M. Cabral Marques, J. Hadgraft, I. W. Kellaway, *Int. J. Pharm.* **1990**, *63*, 259–266.

[17] a) K. S. S. P. Rao, S. M. Hubig, J. N. Moorthy, J. K. Kochi, *J. Org. Chem.* **1999**, *64*, 8098–8104; b) T. Tamaki, T. Kokubu, K. Ichimura, *Tetrahedron* **1987**, *43*, 1485–1494.

[18] G. Grabner, K. Rechthaler, B. Mayer, G. Kohler, K. Rotkiewicz, *J. Phys. Chem. A* **2000**, *104*, 1365–1376.

[19] a) R. A. Agbaria, E. Roberts, I. M. Warner, *J. Phys. Chem.* **1995**, *99*, 10056–10060; b) Y. Chen, Y. Tao, H. Lin, *Macromolecules* **2006**, *39*, 8559–8566.

[20] N. Miyakawa, T. Kiba, S. I. Sato, *Mol. Cryst. Liq. Cryst.* **2010**, *520*, 469–476.

[21] a) K. Kano, H. Matsumoto, S. Hashimoto, M. Sisido, Y. Imanishi, *J. Am. Chem. Soc.* **1985**, *107*, 6117–6118; b) T. Yorozu, M. Hoshino, M. Imamura, *J. Phys. Chem.* **1982**, *86*, 4426–4429.

[22] A. Müller, G. Wenz, *Chem. Eur. J.* **2007**, *13*, 2218–2223.

[23] K. Harata, *Bull. Chem. Soc. Jpn.* **1987**, *60*, 2763–2767.

[24] Gaussian 03, Revision E.01, M. J. Frisch, G. W. Trucks, H. B. Schlegel, G. E. Scuseria, M. A. Robb, J. R. Cheeseman, J. A. Montgomery, T. Vreven, K. N. Kudin, J. C. Burant, J. M. Millam, S. S. Iyengar, J. Tomasi, V. Barone, B. Mennucci, M. Cossi, G. Scalmani, N. Rega, G. A. Petersson, H. Nakatsuji, M. Hada, M. Ehara, K. Toyota, R. Fukuda, J. Hasegawa, M. Ishida, T. Nakajima, Y. Honda, O. Kitao, H. Nakai, M. Klene, X. Li, J. E. Knox, H. P. Hratchian, J. B. Cross, V. Bakken, C. Adamo, J. Jaramillo, R. Gomperts, R. E. Stratmann, O. Yazyev, A. J. Austin, R. Cammi, C. Pomelli, J. W. Ochterski, P. Y. Ayala, K. Morokuma, G. A. Voth, P. Salvador, J. J. Dannenberg, V. G. Zakrzewski, S. Dapprich, A. D. Daniels, M. C. Strain, O. Farkas, D. K. Malick, A. D. Rabuck, K. Raghavachari, J. B. Foresman, J. V. Ortiz, Q. Cui, A. G. Baboul, S. Clifford, J. Cioslowski, B. B. Stefanov, G. Liu, A. Liashenko, P. Piskorz, I. Komaromi, R. L. Martin, D. J. Fox, T. Keith, A. Laham, C. Y. Peng, A. Nanayakkara,

M. Challacombe, P. M. W. Gill, B. Johnson, W. Chen, M. W. Wong, C. Gonzalez, J. A. Pople, Gaussian , Inc., Wallingford, CT, **2004**.
[25] C. Gonzalez, E. C. Lim, *J. Phys. Chem. A* **2000**, *104*, 2953–2957.
[26] S. Grimme, *Angew. Chem.* **2008**, *120*, 3478–3483; *Angew. Chem. Int. Ed.* **2008**, *47*, 3430–3434.
[27] K. Guckian, B. Schweitzer, X. Rex, C. Sheils, D. Tahmassebi, E. Kool, *J. Am. Chem. Soc.* **2000**, *122*, 2213–2222.
[28] J. Mizoguchi, Y. Kawanami, T. Wada, K. Kodama, K. Anzai, T. Yanagi, Y. Inoue, *Org. Lett.* **2006**, *8*, 6051–6054.
[29] A. W. Snow, E. E. Foos, *Synthesis* **2003**, 0509–0512.
[30] H. Lund, J. Bjerrum, *Chem. Ber.* **1931**, *64*, 210–213.
[31] a) S. Nigam, G. Durocher, *J. Phys. Chem.* **1996**, *100*, 7135–7142; b) G. Cox, N. Turro, N. Yang, M. Chen, *J. Am. Chem. Soc.* **1984**, *106*, 422–424.
[32] M. E. Brewster, R. Vandecruys, J. Peeters, P. Neeskens, G. Verreck, T. Loftsson, *Eur. J. Pharm. Sci.* **2008**, *34*, 94–103.
[33] H. Takeru, L. L. John, *J. Am. Pharm. Assoc.* **1954**, *43*, 349–354.
[34] a) D. Holmes, S. Kumaraswamy, A. Matzger, K. Vollhardt, *Chem. Eur. J.* **1999**, *5*, 3399–3412; b) J. Bouwstra, A. Schouten, J. Kroon, *Acta Crystallogr. Sect. C* **1984**, *40*, 428–431; c) V. Petrícek, I. Císarová, L. Hummel, J. Kroupa, B. Brezina, *Acta Crystallogr. Sect. B* **1990**, *46*, 830–832; d) A. C. Blackburn, L. J. Fitzgerald, R. Gerkin, *Acta Crystallogr. Sect. C* **1996**, *52*, 2862–2864; e) J. Oddershede, S. Larsen, *J. Phys. Chem. A* **2004**, *108*, 1057–1063; f) J. Robertson, H. Shearer, G. Sim, D. Watson, *Acta Crystallogr.* **1962**, *15*, 1–8; g) C. Brock, J. Dunitz, *Acta Crystallogr. Sect. B* **1990**, *46*, 795–806; h) T. Welberry, *Proc. R. Soc. London Ser. A* **1973**, *334*, 19–48.
[35] K. Lindner, W. Saenger, *Carbohydr. Res.* **1982**, *99*, 103–115.
[36] a) J. J. P. Stewart, *J. Comput. Chem.* **1989**, *10*, 209–220; b) J. J. P. Stewart, *J. Comput. Chem.* **1989**, *10*, 221–264.
[37] W. Humphrey, A. Dalke, K. Schulten, *J. Mol. Graph.* **1996**, *14*, 33–38.
[38] S. F. Boys, F. Bernardi, *Mol. Phys.* **1970**, *19*, 553–566.

Received: March 1, 2011
Published online: July 7, 2011

